Supplementary material

A robust framework for comparing Lagrangian and gridded Eulerian velocity fields: an example application to surface drifters and altimetry-derived surface currents

Arthur Coquereau[1, 2] and Nicholas P. Foukal[2]

[1]Laboratoire d'Océanographie Physique et Spatiale, Univ. Brest CNRS IRD Ifremer, Brest, France
[2]Woods Hole Oceanographic Institution, Woods Hole, MA 02543, USA

Correspondence: Arthur Coquereau (arthur.coquereau@univ-brest.fr)

Section 1 - Drifter Data Processing

Drifter trajectories have been processed to detect and remove outliers and non-significant data.

First, in the present study, we use the southern tip of Greenland, between the deployment area on the Southeast Greenland Shelf and Cape Desolation on the Southwest Greenland Shelf (49°W-41°W, 59°N-62°N) (Fig. 4). Only data inside the area
5 are used for this validation. Second, the presence of drogues is checked. The most common source of failure in a surface drifter is the tether disconnecting from the drogue or the surface buoy. This arises because either the surface buoy is experiencing a different wave field than the drogue and the tether is put under repeated tension until it breaks, or from interactions with the coastline where rocks can sever the tether. If the drogue detaches, we do not use any further the data. Three different analyses are performed to identify drogue losses. (1) Based on visual analysis, collisions with the coast are detected and flagged. (2)
10 Buoy parameters (submergence count and GPS Time To First Fix) are analyzed according to Drifter Management Team (2018) manual by detecting unusual values. Here, only drifters undergoing repeated collisions with the coast show anomalous values, which are usually repeated low values. (3) The coefficient of determination R^2 between complex drifter velocity U and complex wind velocity W (from ERA5 Hersbach et al., 2020) or similarly the least-square complex linear regression of drifter velocity from wind velocity (Kundu, 1976; Poulain et al., 2009) is computed. The mean R^2 obtained is 3.3% and the maximum 9.6%.
15 Poulain et al. (2009) obtained coefficients of determination for undrogued drifters of 21-22%. We can thus consider our drifters as drogued while they are in the region of interest for this study. This result is expected given that drifters had been deployed within the past 1-2 months and typically drifters lose their drogues after months or years of repeated wear and tear.

Another reason for discarding data in our study region is that drifters around Greenland can enter the fjords. The sections of trajectories concerned have also been flagged and trajectories have been completely removed from the investigation if the
20 drifter remains inside a fjord during the entire experiment. Abnormal locations due to drifter testing prior to deployment are also flagged. In total, 4 trajectories have been removed (3 GFWE + 1 TERIFIC) from our investigations and 16 sections of drifter trajectories have been flagged (6 GFWE + 10 TERIFIC). The presence of outliers has also been evaluated, as suggested

in Elipot et al. (2016), detecting longitude or latitude peaks greater (smaller) than a 5-point median filter + (-) 5 standard deviations. These jumps can arise from errors in GPS fixes, but no such outliers have been detected in the data set.

25   The higher frequency contributions to motion that are not resolved in the evaluated fields (e.g. inertial oscillations and tide) have been removed using a low-pass filter. We assume that these contributions have a negligible impact on the general pathways of water parcels, and we do not expect the altimetry fields to resolve these scales. For instance, following Cushman-Roisin (1982), at 60 ° latitude and with velocity V order of 1 m.s^{-1}, the contribution of inertial oscillations to the westward motion scales as $-\beta V^2/2f_0^2$ which is order 10^{-4}m.s^{-1}.rad^{-1} and can therefore be neglected. A 4th order Butterworth filter

30   with a cut-off frequency of 24 hours has been applied on latitude and longitude time series. This cut-off frequency of 24 hours was chosen to remove most of inertial frequencies (T = 13.8 hours at 60°N) and semidiurnal tides. Smoothing at longer periods to remove the diurnal tides was also tested but part of the cross-shelf structure of the trajectories was lost because some of the synoptic wind forcing was acting at similar time scales. Thus 24 hours was a good balance for the validation between removing much of the periodic motions while retaining the general character of the drifter trajectories.

35   Finally, zonal and meridional components of velocity have been calculated from longitudes and latitudes via a centered finite difference that averages the displacement between the previous and the following hourly locations. We then applied the 3 m.s^{-1} abnormal threshold velocity criterion (Elipot et al., 2016), but found no velocities that exceeded this threshold. It seemed interesting to evaluate the impact of waves on the drifter trajectories. for this, we calculated the coefficient of determination between drifter velocities and a Stoke's drift product (from wave model MFWAM, doi:10.48670/moi-00017). The analysis

40   returns a low R^2 around 5% in average, implicating a very small impact of waves on trajectories.

As explained by Davis (1991), the inhomogeneity of sampling can induce an "array bias". Indeed, in the case where all the drifters are deployed in a small geographic region, a gradient of drifter concentration exists, and the mass diffusivity will tend to produce an apparent drift toward the low concentration region even in absence of mean flow. To test whether the data set could be influenced by this bias, a Peclet number has been computed to evaluate the relative importance of advection

45   compared to diffusion and dispersion. For each line, the dispersion of the drifter related to the center of mass of the line and the distance travelled are computed. The Peclet numbers obtained are always greater than one after deployment, which indicates that advection dominates. The array bias is therefore neglected in the work.

Section 2 - Temporal scope extending

One of the main limitations of this study is its temporal extension. Indeed, this deployment offers a relatively large spatial

50   sampling and a good statistical significance with 38 drifters traveling the area almost at the same time. However, the average travelled time of drifters around the area is 21 days. Therefore, it is not sufficient to conclude about the general consistency of the altimetry-derived surface currents. In particular our data covers from mid August to September, knowing that the strong winter wind conditions play a role on the cross-shelf dynamics, it is crucial to have an idea of the consistency over a longer period and various seasons. The GDP Global surface drifter data set at 6-hourly resolution (Lumpkin and Centurioni, 2019)

55   has therefore been employed to investigate the trajectories of drifters from other deployments traveling the area. 34 drifter
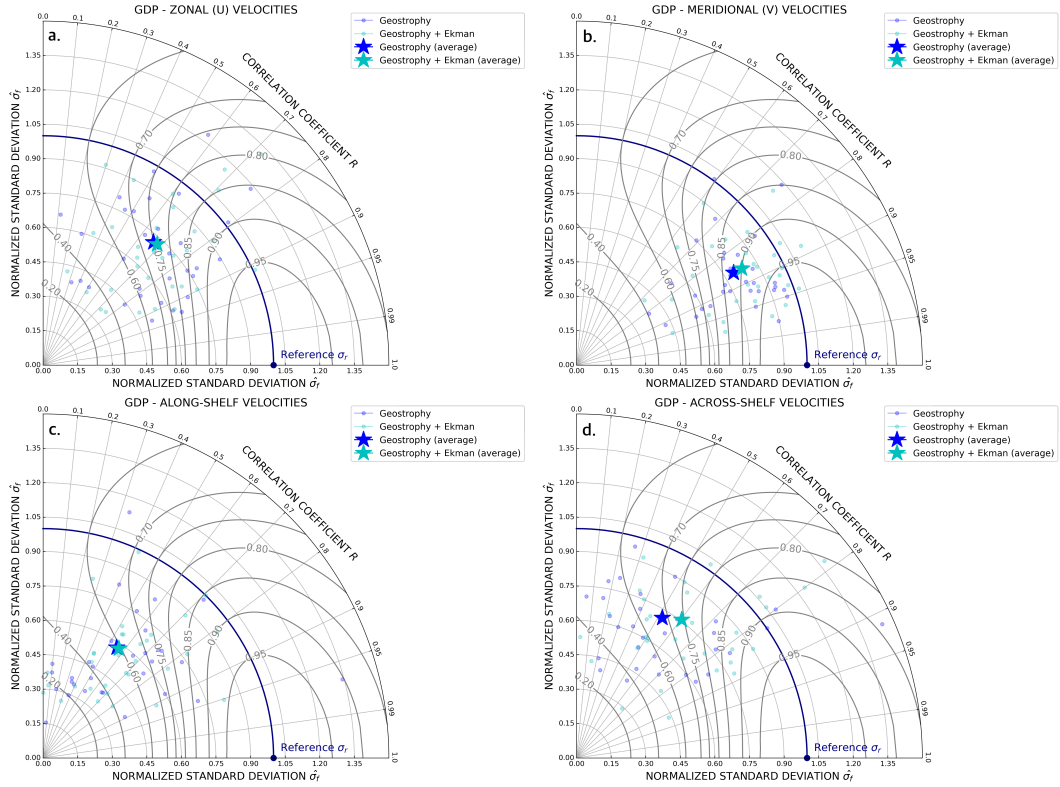
Figure S 1. Taylor diagrams of velocities derived from ADSC products along GDP drifter trajectories. Different velocity components have been evaluated: (a) Zonal, (b) Meridional, (c) Along- shelf and (d) Across-shelf for Gesotrophy product (light blue) and Geostrophy+Ekman (dark blue). A detailed explanation of Taylor diagrams is provided in Fig. 4. The Taylor diagrams presented here are modified versions of an initial Python code by Copin (2012)

trajectories have been collected on the East Greenland Shelf from 1993 to 2020, but no drifters were present before 1996. The three-step methodology presented in the main body of the article was similarly applied to this data set.

The point-wise comparison (Fig. S1) presents good skill scores (Table S1) comparable to those obtained with GFWE+TERIFIC drifters data set. The results for the across-shelf component are even better.

60   Concerning the Eulerian gridding, the direction of currents (Fig. S2) are once again very well resolved with a mean angle between drifters' directions and Geostrophy+Ekman directions around 10.1°. The magnitude of currents is less well resolved than the direction for this data set as well, but the errors are smaller than with GFWE+TERIFIC drifters, with a mean absolute error of 23.8%.

Finally, the synthetic trajectories (Fig. S3) show also good results, lower to those obtained with the previous set of drifters
65   but comparable to those obtained by Liu et al. (2014) on the shelf (0.41). The mean skill score obtained is 0.39 (a). Looking at the distribution of skill scores by months (b) and years (c), we can see that the results previously presented (in orange) are quite

Taylor Skill Score		
	Geostrophy	Geostrophy+Ekman
Zonal (u)	0.75	0.76
Meridional (v)	0.88	0.90
Along-shelf	0.58	0.59
Across-shelf	0.68	0.74

Table S 1. Taylor Skill Score obtained for the two Eulerian products and for the different velocity component
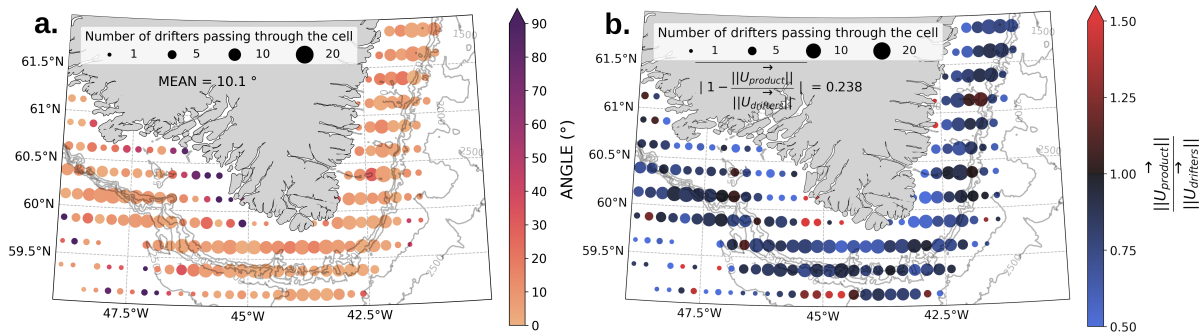
Figure S 2. Comparison of mean flow obtained from GDP drifter trajectories and Geostrophy+Ekman product. Two aspects are evaluated: the angle between drifter directions and directions from ADSC (a) and the ratio of the drifter velocities over ADSC velocities (b)

consistent with the results obtained here at different seasons, for different months and years. However, the months of October and December and the years 1996 and 2019 show lower skill scores, but these results could be not significant because the surrounding periods are not showing such low scores. Overall, this slight improvement in two of the three evaluative metrics with the GDP data set is surprising because the density of satellite altimeters has increased over time. So, one would think that the more recent deployments would yield higher comparative metrics. We posit that the reason for this improvement is due to stronger winds in non-summer months driving stronger ocean currents that can be more accurately measured by remote sensing. We acknowledge that we do not detect a clear seasonal bias in our GDP results here, but sparse sampling likely plays a role in this lack of signal.
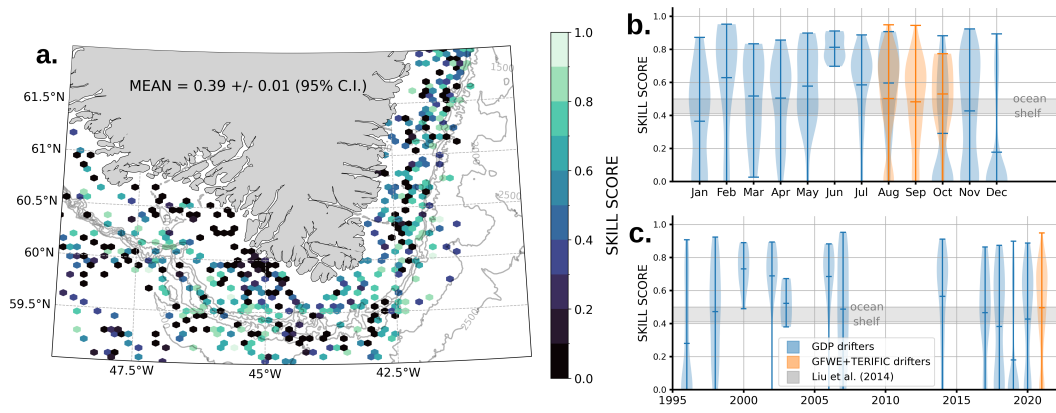
Figure S 3. Synthetic and observed trajectories comparison applied to GDP data set and Geostrophy+Ekman product. (a) Map of skill scores obtained. Confidence interval is computed using Bootstrap methodology. On the right panels, violin plots present the distribution of skill scores obtained by months (b) and years (c). Violin plots are similar to box plots with the addition of probability density curves on each side to represent the distribution of skill scores and the relative importance of a given score compared to other scores obtained.

75   **Section 3 - Comparison between time averaging and synchronous methodology for computing average Eulerian flows**
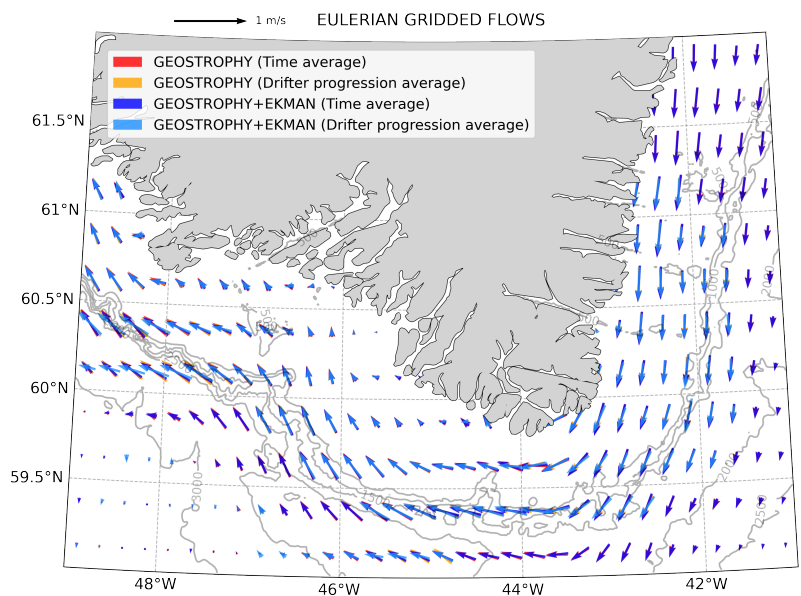
Figure S 4. Comparison of Geostrophy and Geostrophy+Ekman velocity fields computed with a simple time average or with our proposed methodology allowing to mimic the progressive sampling by drifters.

References

Copin, Y.: Taylor diagram for python/matplotlib, https://doi.org/10.5281/zenodo.5548061, language: eng, 2012.

Cushman-Roisin, B.: Motion of a free particle on a beta-plane, Geophysical & Astrophysical Fluid Dynamics, 22, 85–102, https://doi.org/10.1080/03091928208221738, publisher: Taylor & Francis _eprint: https://doi.org/10.1080/03091928208221738, 1982.

Davis, R. E.: Observing the general circulation with floats, Deep Sea Research Part A. Oceanographic Research Papers, 38, S531–S571, https://doi.org/10.1016/S0198-0149(12)80023-9, 1991.

Elipot, S., Lumpkin, R., Perez, R. C., Lilly, J. M., Early, J. J., and Sykulski, A. M.: A global surface drifter data set at hourly resolution, Journal of Geophysical Research: Oceans, 121, 2937–2966, https://doi.org/10.1002/2016JC011716, _eprint: https://onlinelibrary.wiley.com/doi/pdf/10.1002/2016JC011716, 2016.

Hersbach, H., Bell, B., Berrisford, P., Hirahara, S., Horányi, A., Muñoz-Sabater, J., Nicolas, J., Peubey, C., Radu, R., Schepers, D., Simmons, A., Soci, C., Abdalla, S., Abellan, X., Balsamo, G., Bechtold, P., Biavati, G., Bidlot, J., Bonavita, M., De Chiara, G., Dahlgren, P., Dee, D., Diamantakis, M., Dragani, R., Flemming, J., Forbes, R., Fuentes, M., Geer, A., Haimberger, L., Healy, S., Hogan, R. J., Hólm, E., Janisková, M., Keeley, S., Laloyaux, P., Lopez, P., Lupu, C., Radnoti, G., de Rosnay, P., Rozum, I., Vamborg, F., Villaume, S., and Thépaut, J.-N.: The ERA5 global reanalysis, Quarterly Journal of the Royal Meteorological Society, 146, 1999–2049, https://doi.org/10.1002/qj.3803, _eprint: https://onlinelibrary.wiley.com/doi/pdf/10.1002/qj.3803, 2020.

Kundu, P. K.: Ekman Veering Observed near the Ocean Bottom, Journal of Physical Oceanography, 6, 238–242, https://doi.org/10.1175/1520-0485(1976)006<0238:EVONTO>2.0.CO;2, publisher: American Meteorological Society Section: Journal of Physical Oceanography, 1976.

Liu, Y., Weisberg, R. H., Vignudelli, S., and Mitchum, G. T.: Evaluation of altimetry-derived surface current products using Lagrangian drifter trajectories in the eastern Gulf of Mexico, Journal of Geophysical Research: Oceans, 119, 2827–2842, https://doi.org/10.1002/2013JC009710, _eprint: https://onlinelibrary.wiley.com/doi/pdf/10.1002/2013JC009710, 2014.

Lumpkin, R. and Centurioni, L.: NOAA Global Drifter Program quality-controlled 6-hour interpolated data from ocean surface drifting buoys., https://doi.org/10.25921/7ntx-z961, type: dataset; Accessed 2022/12/06, 2019.

Poulain, P.-M., Gerin, R., Mauri, E., and Pennel, R.: Wind Effects on Drogued and Undrogued Drifters in the Eastern Mediterranean, Journal of Atmospheric and Oceanic Technology, 26, 1144–1156, https://doi.org/10.1175/2008JTECHO618.1, publisher: American Meteorological Society Section: Journal of Atmospheric and Oceanic Technology, 2009.

Team, D. D. M.: Drifting buoys DAC data quality control manual, https://archimer.ifremer.fr/doc/00409/52040/, 2018.